arXiv:1702.06084v1 [math.DS] 20 Feb 2017

Newton flows for elliptic functions IV

Pseudo Newton graphs: bifurcation & creation of flows

G.F. Helminck,
Korteweg-de Vries Institute
University of Amsterdam
P.O. Box 94248
1090 GE Amsterdam
The Netherlands
e-mail: g.f.helminck@uva.nl
F. Twilt,
Department of Applied Mathematics
University of Twente
P.O. Box 217, 7500 AE Enschede
The Netherlands
e-mail: f.twilt@kpnmail.nl

February 21, 2017

Abstract

An elliptic Newton flow is a dynamical system that can be interpreted as a continuous version of Newton's iteration method for finding the zeros of an elliptic function f. Previous work focusses on structurally stable flows (i.e., the phase portraits are topologically invariant under perturbations of the poles and zeros for f), including a classification / representation result for such flows in terms of *Newton graphs* (i.e., cellularly embedded toroidal graphs fulfilling certain combinatorial properties). The present paper deals with *non-structurally stable elliptic Newton flows* determined by pseudo Newton graphs (i.e., cellularly embedded toroidal graphs, either generated by a Newton graph, or the so called nuclear Newton graph, exhibiting only one vertex and two edges). Our study results into a deeper insight in the creation of structurally stable Newton flows and the bifurcation of non-structurally stable Newton flows.

Subject classification: 05C75, 33E05, 34D30, 37C70, 49M15.

Keywords: Dynamical system, desingularized elliptic Newton flow, structural stability, elliptic function, phase portrait, Newton graph (elliptic-, nuclear-, pseudo-), cellularly embedded toroidal (distinguished) graph, face traversal procedure, Angle property, Euler property, Hall condition.

1 Motivation; recapitulation of earlier results

In order to clarify the context of the present paper, we recapitulate some earlier results.

1.1 Elliptic Newton flows; structural stability

The results in the following four subsections, can all be found in our paper [2].

1.1.1 Planar and toroidal elliptic Newton flows

Let f be an elliptic (i.e., meromorphic, doubly periodic) function of order $r(\geqslant 2)$ on the complex plane $\mathbb{C}$ with $(\omega_1,\ \omega_2)$, $\mathrm{Im}\frac{\omega_2}{\omega_1} > 0$, as *basic periods* spanning a lattice $\Lambda(=\Lambda_{\omega_1,\,\omega_2})$.

The *planar elliptic Newton flow* $\overline{\mathcal{N}}(f)$ is a C^1-vector field on $\mathbb{C}$, defined as a *desingularized version*[1] of the planar dynamical system, $\mathcal{N}(f)$, given by:

$$\frac{dz}{dt} = \frac{-f(z)}{f'(z)}, z \in \mathbb{C}. \tag{1}$$

On a non-singular, oriented $\overline{\mathcal{N}}(f)$-trajectory $z(t)$ we have:

- arg (f) =constant, and $|f(z(t))|$ is a strictly decreasing function on t.
So that the $\overline{\mathcal{N}}(f)$-*equilibria* are of the form:
- a stable star node (attractor); in the case of a zero for f, or
- an unstable star node (repellor); in the case of a pole for f, or
- a saddle; in the case of a critical point for f (i.e., f' vanishes, but f not).

For an (un)stable node the (outgoing) incoming trajectories intersect under a non-vanishing angle $\frac{\Delta}{k}$, where Δ stands for the difference of the arg$f$-values on these trajectories, and k for the multiplicity of the corresponding (pole) zero. The saddle in the case of a *simple* critical point (i.e., f' does not vanish) is *orthogonal* and the two unstable (stable) separatrices constitute the "local" *unstable (stable) manifold* at this saddle.

Functions such as f correspond to meromorphic functions on the torus $T(\Lambda)(=\mathbb{C}/\Lambda_{\omega_1,\,\omega_2})$. So, we can interprete $\overline{\mathcal{N}}(f)$ as a global C^1-vector field, denoted[2] $\overline{\overline{\mathcal{N}}}(f)$, on the Riemann surface $T(\Lambda)$ and it is allowed to apply results for C^1-vector fields on compact differential manifolds, such as certain theorems of Poincaré-Bendixon-Schwartz (on limiting sets) and those of Baggis-Peixoto (on C^1-structural stability).
It is well-known that the function f has precisely r zeros and r poles (counted by multiplicity) on the half open / half closed period parallelogram $P_{\omega_1,\,\omega_2}$ given by

$$\{t_1\omega_1 + t_2\omega_2 \mid 0 \leqslant t_1 < 1,\ 0 \leqslant t_2 < 1\}.$$

Denoting these zeros and poles by $a_1,\cdots,a_r$, resp. $b_1,\cdots,b_r$, we have[3]: (cf. [8])

$$a_i \neq b_j, i,j = 1,\cdots,r \text{ and } a_1 + \cdots + a_r = b_1 + \cdots + b_r + \lambda_0, \lambda_0 \in \Lambda, \tag{2}$$

and thus

$$[a_i] \neq [b_j], i,j = 1,\cdots,r \text{ and } [a_1] + \cdots + [a_r] = [b_1] + \cdots + [b_r]. \tag{3}$$

where $[a_1],\cdots,[a_r]$ and $[b_1],\cdots,[b_r]$ are the zeros, resp. poles for f on $T(\Lambda)$ and $[\cdot]$ stands for the congruency class mod Λ of a number in $\mathbb{C}$. Conversely, any pair $(\{a_1,\cdots,a_r\},\{b_1,\cdots,b_r\})$

[1] In fact, we consider the system $\frac{dz}{dt} = -(1+|f(z)|^4)^{-1}|f'(z)|^2\frac{f(z)}{f'(z)}$: a continuous version of Newton's damped iteration method for finding zeros for f.

[2] Occasionally, we will refer to $\overline{\mathcal{N}}(f)$ as to a toroidal (elliptic) Newton flow.

[3] In fact $\lambda_0 = -\eta(f(\gamma_2))\omega_1 + \eta(f(\gamma_1))\omega_2$, where $\eta(f(\cdot))$ stands for winding numbers of the curves $f(\gamma_1)$ and $f(\gamma_2)$ with γ_i the sides of $P_{\omega_1,\,\omega_2}$ spanned by $\omega_i, i = 1,2$, (cf. [10]).

that fulfils (2) determines (up to a multiplicative constant) an elliptic function with $\{a_1,\cdots,a_r\}$ and $\{b_1,\cdots,b_r\}$ as zeros resp. poles in $P(=P_{\omega_1,\,\omega_2})$.

1.1.2 The topology τ_0

It is not difficult to see that the functions f, and also the corresponding toroidal Newton flows, can be represented by the set of all ordered pairs $(\{[a_1],\cdots,[a_r]\},\{[b_1],\cdots,[b_r]\})$ of congruency classes mod Λ (with $a_i,b_i\in P, i=1,\ldots,r,$) that fulfil (3).

This representation space can be endowed with a topology, say τ_0, induced by the Euclidean topology on $\mathbb{C}$, that is natural in the following sense: Given an elliptic function f of order r and $\varepsilon>0$ sufficiently small, a τ_0-neighborhood $\mathcal{O}$ of f exists such that for any g in $\mathcal{O}$, the zeros (poles) for g are contained in ε-neighborhoods of the zeros (poles) for f.

$E_r(\Lambda)$ is the set of all functions f of order r on $T(\Lambda)$ and $N_r(\Lambda)$ the set of corresponding flows $\overline{\overline{\mathcal{N}}}(f)$. By $X(T)$ we mean the set of all C^1-vector fields on T, endowed with the C^1-topology (cf. [6]).

The topology τ_0 on $E_r(\Lambda$ and the C^1-topology on $X(T)$ are matched by:

The map $E_r(\Lambda)\to X(T):f\mapsto\overline{\overline{\mathcal{N}}}(f)$ is τ_0-C^1 continuous.

1.1.3 Canonical forms of elliptic Newton flows

The flows $\overline{\overline{\mathcal{N}}}(f)$ and $\overline{\overline{\mathcal{N}}}(g))$ in $N_r(\Lambda)$ are called *conjugate*, denoted $\overline{\overline{\mathcal{N}}}(f)\sim\overline{\overline{\mathcal{N}}}(g)$, if there is a homeomorphism from T onto itself mapping maximal trajectories of $\overline{\overline{\mathcal{N}}}(f)$ onto those of $\overline{\overline{\mathcal{N}}}(g)$, thereby respecting the orientations of these trajectories.

For a given f in $E_r(\Lambda)$, let the lattice Λ^* be arbitrary. Then there is a function f^* in $E_r(\Lambda^*)$ such that:

$$\overline{\overline{\mathcal{N}}}(f)\sim\overline{\overline{\mathcal{N}}}(f^*).$$

In fact, the linear isomorphism $\mathbb{C}\to\mathbb{C}:(\omega_1,\omega_2)\mapsto(\omega_1^*,\omega_2^*)$; $\mathrm{Im}\frac{\omega_2^*}{\omega_1^*}>0$, transforms Λ into Λ^* and the pair $(\{a_1,\cdots,a_r\},\{b_1,\cdots,b_r\})$, determining f, into $(\{a_1^*,\cdots,a_r^*\},\{b_1^*,\cdots,b_r^*\})$ fixing f^* in $E_r(\Lambda^*)$; if $\Lambda=\Lambda^*$, then this linear isomorphism is unimodular.
It is always possible to choose[4] $\Lambda^*(=\Lambda_{1,\tau})$, where $(1,\tau)$ is a *reduced*[5] pair of periods for f^* and to subsequently apply the linear transformation $(1,\tau)\mapsto(1,i)$, so that we even may assume that $(1,i)$ is a pair of reduced periods for the corresponding elliptic function on $\Lambda_{1,i}$.

Consequently, unless strictly necessary, we suppress the role of Λ and write: $E_r(\Lambda)=E_r$, $T(\Lambda)=T$ and $N_r(\Lambda)=N_r$.

1.1.4 Structural stability

The flow $\overline{\overline{\mathcal{N}}}(f)$ in N_r is called τ_0-*structurally stable*, if there is a τ_0-neighborhood $\mathcal{O}$ of f, such that for all $g\in\mathcal{O}$ we have: $\overline{\overline{\mathcal{N}}}(f)\sim\overline{\overline{\mathcal{N}}}(g)$; the set of all τ_0-structurally stable flows $\overline{\overline{\mathcal{N}}}(f)$ is denoted by $\tilde{N}_r$.

C^1-structural stability for $\overline{\overline{\mathcal{N}}}(f)$ implies τ_0-structurally stability for $\overline{\overline{\mathcal{N}}}(f)$; see Subsubsection 1.1.2. So, when discussing structurally stable toroidal Newton flows we skip the adjectives

[4] τ satisfies $\mathrm{Im}\ \tau>0, |\tau|\geqslant 1, -\frac{1}{2}\leqslant\mathrm{Re}\ \tau<\frac{1}{2}, \mathrm{Re}\ \tau\leqslant 0,$ if $|\tau|=1$.

[5] A pair (ω_1^*,ω_2^*) of basic periods for f^* is called *reduced* if $|\omega_1^*|$ is minimal among all periods for f^* , whereas $|\omega_2^*|$ is minimal among all periods ω for f^* with the property $\mathrm{Im}\frac{\omega}{\omega_1^*}>0$.

τ_0 and C^1.

- A structurally stable $\overline{\overline{\mathcal{N}}}(f)$ has precisely $2r$ different simple saddles (all orthogonal).

Note that if $\overline{\overline{\mathcal{N}}}(f)$ is structurally stable, then also $\overline{\overline{\mathcal{N}}}(\frac{1}{f})$, because $\overline{\overline{\mathcal{N}}}(\frac{1}{f}) = -\overline{\overline{\mathcal{N}}}(f)$ [**duality**].

The main results obtained in [2] are:

- $\overline{\overline{\mathcal{N}}}(f) \in \tilde{N}_r$ if and only if the function f is non-degenerate[6] [**characterization**].
- The set of all non-degenerate functions of order r is open and dense in E_r [**genericity**].

1.2 Classification & representation of structurally stable elliptic Newton flows

The following three subsubsections describe shortly the main results from our paper [3].

1.2.1 The graphs $\mathcal{G}(f)$ and $\mathcal{G}^*(f)$

For the flow $\overline{\overline{\mathcal{N}}}(f)$ in $\tilde{N}_r$, we define the connected (multi)graph[7] $\mathcal{G}(f)$ of order r on T by:

-vertices are the r zeros for f;
-edges are the $2r$ unstable manifolds at the critical points for f;
-faces are the r basins of repulsion of the poles for f.

Similarly, we define the toroidal graph $\mathcal{G}^*(f)$ at the *repellors, stable manifolds* and *basins of attraction* for $\overline{\overline{\mathcal{N}}}(f)$. Apparently, $\mathcal{G}^*(f)$ is the *geometrical dual* of $\mathcal{G}(f)$; see Fig. 1.

The following features of $\mathcal{G}(f)$ reflect the main properties of the phase portraits of $\overline{\overline{\mathcal{N}}}(f)$:

- $\mathcal{G}(f)$ is **cellularly embedded**, i.e., each face is homeomorphic to an open $\mathbb{R}^2$-disk;
- all (anti-clockwise measured) angles at an attractor in the boundary of a face that span a sector of this face, are strictly positive and sum up to 2π; [**A-property**]
- the boundary of each $\mathcal{G}(f)$-face - as subgraph of $\mathcal{G}(f)$ - is *Eulerian*, i.e., admits a closed facial walk that traverses each edge only once and goes through all vertices [**E-property**].

The anti-clockwise permutation on the embedded edges at vertices of $\mathcal{G}(f)$ induces a clockwise orientation of the facial walks on the boundaries of the $\mathcal{G}(f)$-faces; see Fig.2. On its turn, the clockwise orientation of $\mathcal{G}(f)$-faces gives rise to a clockwise permutation on the embedded edges at $\mathcal{G}^*(f)$-vertices, and thus to an anti-clockwise orientation of $\mathcal{G}^*(f)$. In the sequel, all graphs of the type $\mathcal{G}(f)$, $\mathcal{G}^*(f)$, are always oriented in this way, see Fig.2. Hence, by duality,

$$\mathcal{G}^*(f) = -\mathcal{G}(\frac{1}{f}). \tag{4}$$

It follows that also $\mathcal{G}^*(f)$ is *cellularly embedded* and fufills the *E-* and *A-property.*

1.2.2 Newton graphs

[6] i.e., all *zeros*, *poles* and *critical points* for f are simple, and no critical points are connected by $\overline{\overline{\mathcal{N}}}(f)$-trajectories.

[7] The graph $\mathcal{G}(f)$ has no loops, basically because the zeros for f are simple.

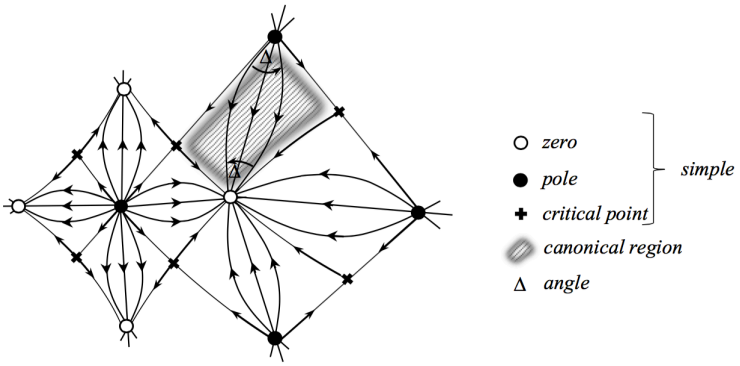

Figure 1: Basin of repulsion (attraction) of $\overline{\overline{\mathcal{N}}}(f)$ for a pole (zero) of f.

A connected multigraph $\mathcal{G}$ in T with r vertices, $2r$ edges and r faces is called *a Newton graph* (of order r) if this graph is *cellularly embedded* and moreover, the *A-property* and the *E-property* hold.
It is proved that the dual $\mathcal{G}^*$ of a Newton graph $\mathcal{G}$ is also *Newtonian* (of order r). The anti-clockwise (clockwise) permutations on the edges of $\mathcal{G}$ at its vertices endow a clockwise (anti-clockwise) orientation of the $\mathcal{G}$-faces and, successively, an anti-clockwise (clockwise) orientation of the $\mathcal{G}^*$-faces, compare Fig.2).

-Apparently $\mathcal{G}(f)$ and $\mathcal{G}^*(f)$ are Newton graphs.

The main results obtained in [3] are:
-If $\overline{\overline{\mathcal{N}}}(f)$ and $\overline{\overline{\mathcal{N}}}(g)$ are structurally stable and of the same order, then:

$$\overline{\overline{\mathcal{N}}}(f) \sim \overline{\overline{\mathcal{N}}}(g) \Leftrightarrow \mathcal{G}(f) \sim \mathcal{G}(g) \text{ [\textbf{classification}]}.$$

-given a clockwise oriented Newton graph $\mathcal{G}$ of order r, there exists a structurally stable Newton flow $\overline{\overline{\mathcal{N}}}(f_{\mathcal{G}})$ such that $\mathcal{G}(f_{\mathcal{G}}) \sim \mathcal{G}$ and thus: ($\mathcal{H}$ is another clockwise oriented Newton graph)

$$\overline{\overline{\mathcal{N}}}(f_{\mathcal{G}}) \sim \overline{\overline{\mathcal{N}}}(f_{\mathcal{H}}) \Leftrightarrow \mathcal{G} \sim \mathcal{H} \text{ [\textbf{representation}]}.$$

Here the symbol $\sim$ between flows stands for conjugacy, and between graphs for equivalency (i.e. an orientation preserving isomorphism).

1.2.3 Characteristics for the A-property and the E-property

Let $\mathcal{G}$ be a cellularly embedded graph of order r in T, not necessarily fulfilling the *A-property*. There is a simple criterion available for $\mathcal{G}$ to fulfil the *A-property*. In order to formulate this criterion, we denote the vertices and faces of $\mathcal{G}$ by v_i and F_j respectively, $i, j = 1, \cdots, r$. Now, let J be a subset of $\{1, \cdots, r\}$ and denote the subgraph of $\mathcal{G}$, generated by all vertices and edges incident with the faces $F_j, j \in J$, by $\mathcal{G}(J)$.The set of all vertices in $\mathcal{G}(J)$ is denoted by $V(\mathcal{G}(J))$. Then:

$\mathcal{G}$ has *the A-property* $\Leftrightarrow$ $|J| < |V(\mathcal{G}(J))|$ for all J, $\emptyset \neq J \subsetneq \{1, \cdots, r\}$, [**Hall condition**]

where $|\cdot|$ stands as usual for cardinality. As a by-product we have:

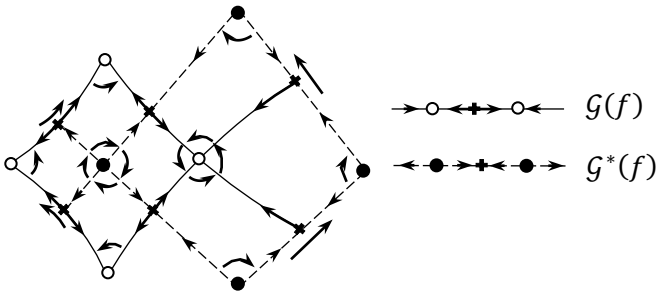

Figure 2: The oriented graphs $\mathcal{G}(f)$ and $\mathcal{G}^*(f)$.

-Under the *A-property*, the set of exterior $\mathcal{G}(J)$-vertices (i.e., vertices in $\mathcal{G}(J)$ that are also adjacent to $\mathcal{G}$-faces, but not in $\mathcal{G}(J)$), is *non-empty.*
-Let $\mathcal{G}$ be a cellularly embedded graph of order r in T, not necessarily fulfilling the *E-property.* We consider the *rotation system* Π for $\mathcal{G}$:

$$\Pi = \{\pi_v \,|\, \text{all vertices } v \text{ in } \mathcal{G}\},$$

where the *local rotation system* π_v at v is the cyclic permutation of the edges incident with v such that $\pi_v(e)$ is the successor of e in the anti-clockwise ordering around v. Then, the boundaries of the faces of $\mathcal{G}$ are formally described by Π-walks as:

If $e(= (v'v''))$ stands for an edge, with end vertices v' and v'', we define a Π-*walk* (*facial walk*), say w, on $\mathcal{G}$ as follows: [**face traversal procedure**]

Consider an edge $e_1 = (v_1v_2)$ and the closed walk $w = v_1e_1v_2e_2v_3\cdots v_ke_kv_1$, which is determined by the requirement that, for $i = 1, \cdots, \ell$, we have $\pi_{v_{i+1}}(e_i) = e_{i+1}$, where $e_{\ell+1} = e_1$ and ℓ is minimal.[8]

Each edge occurs either once in two different Π-walks, or twice (with opposite orientations) in only one Π-walk. $\mathcal{G}$ has the *E-property* iff the first possibility holds for all Π-walks. The dual $\mathcal{G}^*$ admits a loop[9] iff the second possibility occurs at least in one of the Π-walks.
The following observation will be referred to in the sequel:

Under the *E-property* for $\mathcal{G}$, each $\mathcal{G}$-edge is adjacent to different faces; in fact, any $\mathcal{G}$-edge, say e, determines precisely one $\mathcal{G}^*$-edge e^* (and vice versa) so that there are $2r$ intersections $s = (e, e^*)$ of $\mathcal{G}$- and $\mathcal{G}^*$-edges. We consider an abstract graph with these pairs s, together with the $\mathcal{G}$- and $\mathcal{G}^*$-vertices, as vertices, two of the vertices of this abstract graph being connected *iff* they are incident with the same $\mathcal{G}$- edge or $\mathcal{G}^*$-edge. This graph admits a cellular embedding in T (cf. [3]), which will be referred to as to the "distinguished" graph $\mathcal{G} \wedge \mathcal{G}^*$ with as faces the so-called *canonical regions* (compare Fig.3). Following [10], $\mathcal{G} \wedge \mathcal{G}^*$ determines a C^1-structurally stable flow $X(\mathcal{G})$ on T. In [3] we proved that, if the *A-property* holds as well, $X(\mathcal{G})$ is topologically equivalent with a structurally stable elliptic Newton flow of order r.

[8] Apparently, such "minimal" l exists since $\mathcal{G}$ is finite. In fact, the first edge which is repeated in the same direction when traversing w, is e_1 (cf. [9]).
[9] Note that by assumption $\mathcal{G}$ has no loops.

1.3 The Newton graphs of order $r, r = 2, 3$

Following [4], we present the lists of all -up to duality and conjugacy - Newton graphs of order $r, r = 2, 3$.

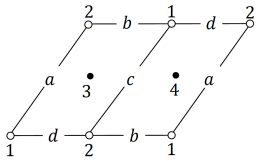

Figure 3: The 2^{nd} order Newton graph.

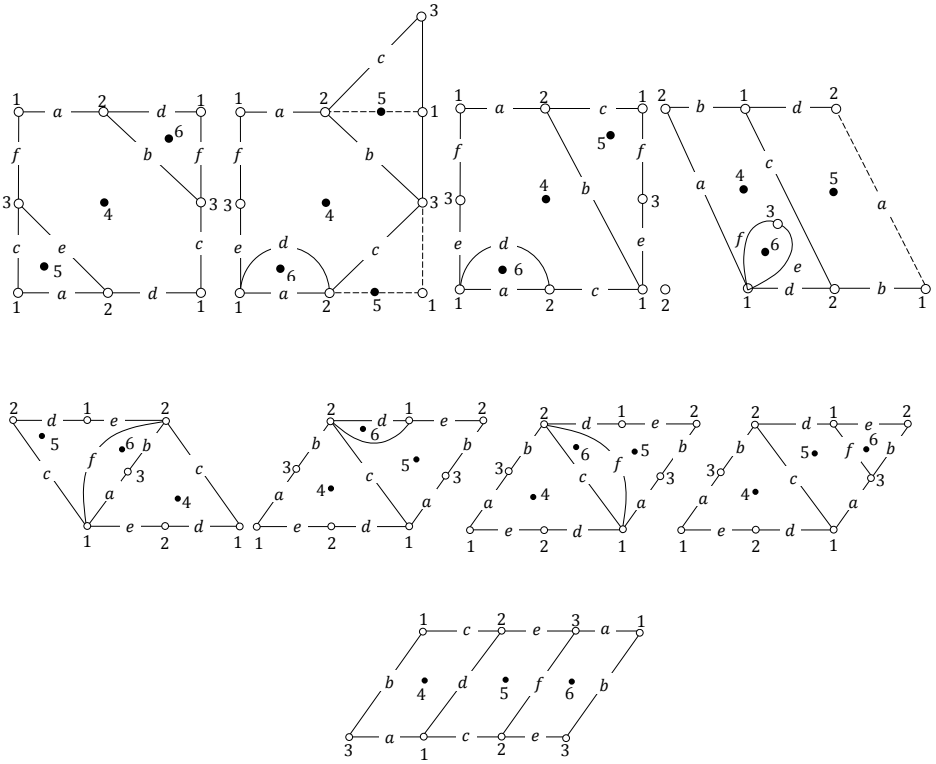

Figure 4: The 3^{rd} order Newton graphs.

2 Pseudo Newton graphs

Throughout this section, let $\mathcal{G}_r$ be a Newton graph of order r.

Due to the *E-property*, we know that an arbitrary edge of $\mathcal{G}_r$ is contained in precisely two different faces. If we delete such an edge from $\mathcal{G}_r$ and merge the involved faces F_1, F_2 into a new face, say $F_{1,2}$, we obtain a toroidal connected multigraph (again cellularly embedded)

with r vertices, $2r-1$ edges and $r-1$ faces: $F_{1,2}$, $F_3, \cdots, F_r$.
If $r=2$, then this graph has only one face.
If $r>2$, put $J=\{1,2\}$, thus $\emptyset \neq J \subsetneq \{1,\cdots,r\}$. Then, we know, by the A-property (cf. Subsubsection 1.2.3) , that the set $\mathrm{Ext}(\mathcal{G}(J))$ of exterior $\mathcal{G}(J)$-vertices is non-empty. Let $v \in \mathrm{Ext}(\mathcal{G}(J))$, thus $v \in \partial F_{1,2}$. Hence, v is incident with an edge, adjacent only to one of the faces F_1, F_2. Delete this edge and obtain the "merged face" $F_{1,2,3}$.
If $r=3$, the result is a graph with only *one* face.

If $r>3$, put $J=\{1,2,3\}$. By the same reasoning as used in the case $r=3$, it can be shown that $\partial F_{1,2,3}$ contains an edge belonging to another face than F_1, F_2 or F_3, say F_4 . Delete this edge and obtain the "merged face" $F_{1,2,3,4}$. And so on. In this way, we obtain - in $r-1$ steps - a connected cellularly embedded multigraph, say $\check{\mathcal{G}}_r$, with r vertices, $r+1$ edges and only one face.

Obviously, $\check{\mathcal{G}}_r$ contains vertices of degree $\geqslant 2$. Let us assume that there exists a vertex for $\check{\mathcal{G}}_r$, say v, with $\deg(v)=1$. If we delete this vertex from $\check{\mathcal{G}}_r$, together with the edge incident with v, we obtain a graph with $(r-1)$ vertices, r edges and *one* face. If this graph contains also a vertex of degree 1, we proceed successively. The process stops after L steps, resulting into a (connected, cellularly embedded) multigraph, say $\hat{\mathcal{G}}_\rho$. This graph admits $\rho = r-L$ vertices (each of degree $\geqslant 2$), $\rho+1$ edges and one face.

Apparently[10] we have: $L<r-1$ and thus $2 \leqslant \rho \leqslant r$. In particular:
if $r=2$, then $\rho=2$ and $L=0$.
if $r=3$, then $\rho=3$ and $L=0$, or $\rho=2$ and $L=1$; see also Fig.5.

From Subsection 1.3, Fig.3, it follows that $\mathcal{G}_2$ is unique (up to equivalency).
From the forthcoming Corollary 2.2 it follows that also $\check{\mathcal{G}}_2$ is unique. However, a graph $\check{\mathcal{G}}_r, r>2$, is not uniquely determined by $\mathcal{G}_r$, as will be clear from Fig.5, where $\mathcal{G}_3$ is a Newton graph (cf. Subsubsection 1.2.3 or Fig.4(iii)).

Lemma 2.1. *For the graphs $\hat{\mathcal{G}}_\rho$ we have:*

(a_1) *Either, two vertices are of degree 3, and all other vertices of degree 2, or*

(a_2) *one vertex is of degree 4, and all other vertices of degree 2.*

(b) *There is a closed, clockwise oriented facial walk, say w, of length $2(\rho+1)$ such that, traversing w, each vertex v shows up precisely $\deg(v)$ times. Moreover, w is divided into subwalks W_1, $W_2, \cdots$, connecting vertices of degree >2 that, apart from these begin- and endpoints, contain only-if any- vertices of degree 2.*

(c_1) *If $e_1 e_2 \cdots e_s$ is a walk of type W_i, then also $W_i^{-1} := e_s^{-1} \cdots e_2^{-1} e_1^{-1}$, where e and e^{-1} stand for the same edge, but with opposite orientation.*

(c_2) *The subwalks W_i and W_i^{-1} are not consecutive in w.*

(c_3) *In Case (a_1), there are precisely 6 subwalks of type W_i, each of them connecting different vertices (of degree 3). In fact there holds: $w = W_1 W_2 W_3 W_1^{-1} W_2^{-1} W_3^{-1}$.*

(c_4) *In Case (a_2), there are precisely 4 subwalks of type W_i , each of them containing at least one vertex of degree 2. In fact we have: $w = W_1 W_2 W_1^{-1} W_2^{-1}$.*

[10] Assume $L=r-1$.Then $\hat{\mathcal{G}}_\rho, \rho=1$, would be a connected subgraph of $\mathcal{G}$, with two edges and one vertex; this contradicts the fact that $\mathcal{G}$ has no loops. Compare the forthcoming Definition 2.5.

Proof. ad (a): Each edge of $\hat{\mathcal{G}}_\rho$ contributes precisely twice to the set $\{\deg(v), v \in V(\hat{\mathcal{G}}_\rho)\}$. It follows:

$$\sum_{\text{all } \hat{\mathcal{G}}_\rho\text{-vertices } v} \deg(v) = 2(\rho+1). \tag{5}$$

Put $k_i = \sharp\{\text{vertices of degree } i\}, i = 1, 2, 3, \cdots$. Then (5) yields:

$$2k_2+3k_3+4k_4+5k_5+\cdots = 2(k_2+k_3+k_4+k_5+\cdots+1)(= 2(\rho+1)).$$

Note that one uses here also that $\hat{\mathcal{G}}_\rho$ has ρ vertices and all these vertices have degree $\geqslant 2$. Thus, either $k_2 = \rho-2, k_3 = 2$, $k_i = 0$ if $i \neq 2, 3$, or $k_2 = \rho-1$, $k_4 = 1$, $k_i = 0$ if $i \neq 2, 4$.

ad (b): The geometrical dual $(\hat{\mathcal{G}}_\rho)^*$ of $\hat{\mathcal{G}}_\rho$ has only one vertex. So, all edges of $(\hat{\mathcal{G}}_\rho)^*$ are loops. Hence, in the *facial* walk w of $\hat{\mathcal{G}}_\rho$, each edge shows up precisely twice (with opposite orientation) cf. Subsubsection 1.2.3. Thus w has length $2(\rho+1)$. By the face traversal procedure, each facial sector of $\hat{\mathcal{G}}_\rho$ is encountered once and -at a vertex v- there are $\deg(v)$ many of such sectors. Application of (a_1) and (a_2) yields the second part of the assertion.

ad (c_1): Let $e_1 v e_2$ be a subwalk of w with $\deg(v) = 2$. Both e_1^{-1} and e_2^{-1} occur precisely once in w, and $e_2^{-1} v e_1^{-1}$ is a subwalk of w.

ad (c_2): If the subwalk $W = e_1 e_2 \cdots e_s$ and its inverse are consecutive, then -by the face traversal procedure- $e_1^{-1} v_1 e_1$, or $e_s v_s e_s^{-1}$ are subwalks of the facial walk w. In the first case, v_1 is both begin- and endpoint of e_1; in the second case, v_s is both begin- and endpoint of e_s. This would imply that $\hat{\mathcal{G}}_\rho$ has a loop which is excluded by construction of this graph.

ad (c_3): Note that, traversing w once, each of the two vertices of degree 3 is encountered thrice. Suppose that the begin en and points of one of the subwalks $W_1, W_2, \cdots$, say W_1, coincide. Then, this also holds for the subwalk W_1^{-1} being-by (c_2)-not adjacent to W_1. So, traversing w once, this common begin/endpoint is encountered at least four times; in contradiction with our assumption. The assertion is an easy consequence of (a_1) and (c_2).

ad (c_4): Traversing w once, the vertex of degree 4 is encountered four times. In view of (a_2) and (c_2), we find four closed subwalks of w namely: W_1, W_1^{-1} (not adjacent) and W_2, W_2^{-1} (not adjacent). Finally we note that each of these subwalks must contain at least one vertex of degree 2 (since $\hat{\mathcal{G}}_\rho$ has no loops). □

An analysis of its rotation system learns that $\hat{\mathcal{G}}_\rho$ is determined by its facial walk w, and thus also by the subwalks $W_1W_2W_3$ (in Case a_1) or W_1W_2 (in Case a_2). In fact, only the length of the subwalks W_i matters.

Corollary 2.2. *The graphs $\hat{\mathcal{G}}_2$ and $\hat{\mathcal{G}}_3$ can be described as follows:*

- *By Lemma 2.1 it follows that $\hat{\mathcal{G}}_2$ does not have a vertex of degree 4. So, $\hat{\mathcal{G}}_2$ is of the form as depicted in Fig.6-a_1, where each subwalk W_i admits only one edge. Hence, there is-up to equivalency- only one possibility for $\hat{\mathcal{G}}_2$. Compare also Fig.3.*

- *It is easily verified that -in Fig.7- each graph (on solid and dotted edges) is a Newton graph (cf. Subsubsection 1.2.3). Hence, in case $\rho = 3$, both alternatives in Lemma 2.1-(a) occur. An analysis of their rotation systems learns that the three graphs with only solid edges in Fig.7-$(i)-(iii)$ are equivalent, but not equivalent with the graph on solid edges in Fig.7-(iv). In a similar way it can be proved that the graphs in Fig.7 expose all possibilities(up to equivalency) for $\hat{\mathcal{G}}_3$.*

Definition 2.3. *Pseudo Newton graphs*
Cellularly embedded toroidal graphs, obtained from $\mathcal{G}_r$ by deleting edges and vertices in the way as described above, are called *pseudo Newton graphs* (of order r).

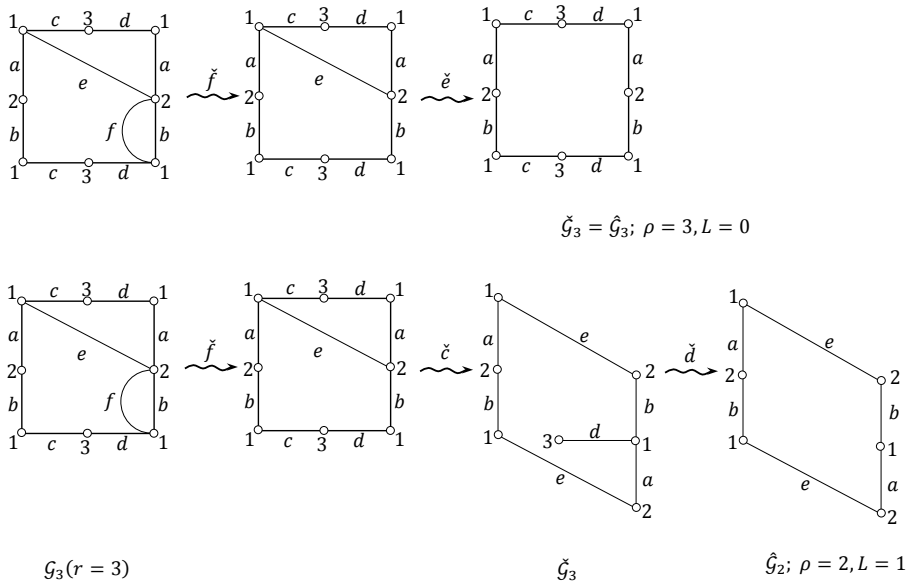

Figure 5: Some graphs $\mathcal{G}_3$, $\check{\mathcal{G}}_3$ and $\hat{\mathcal{G}}_\rho$.

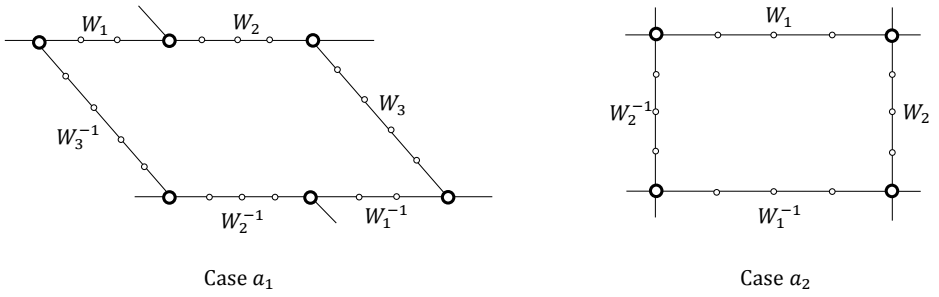

Figure 6: The graphs $\hat{\mathcal{G}}_\rho$.

Apparently, a pseudo Newton graph is not a Newton graph by itself. Replacing (in the inverse order) into $\hat{\mathcal{G}}_\rho, \rho = r - L$, the edges and vertices that we have deleted from $\mathcal{G}_r$, we regain subsequently $\check{\mathcal{G}}_\rho$ and $\mathcal{G}_r$. A pseudo Newton graph of order r has either one face with angles summing up to the number $(\rho^{'})$ of its vertices and $(\rho^{'} + 1)$ edges $(2 \leqslant \rho \leqslant \rho^{'} \leqslant r)$ or one face with angles summing up to $r', r - r'$ faces with angles summing up to 1 and altogether $2r - r' + 1$ edges $(2 \leqslant r, 1 < r' < r)$.

Remark 2.4. If we delete from $\hat{\mathcal{G}}_\rho$ an arbitrary edge, the resulting graph remains connected, but the alternating sum of vertices, edges and face equals +1. Thus one obtains a graph that is not cellularly embedded.

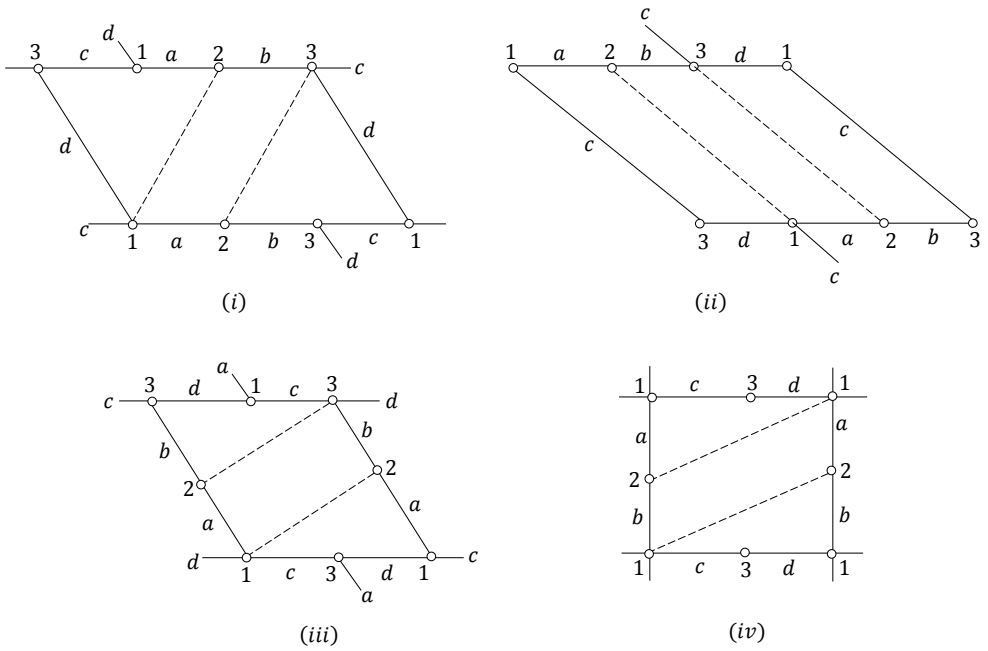

Figure 7: All possible graphs $\hat{\mathcal{G}}_3$.

Definition 2.5. A *Nuclear Newton graph* is a cellularly embedded graph in T with one vertex and two edges.

Apparently a Nuclear Newton graph is connected and admits one face and two loops. In particular such a graph has a trivial rotation system. Hence, all nuclear Newton graphs are topologically equivalent and since they expose the same structure as the pseudo Newton graphs $\hat{\mathcal{G}}_\rho$, they will be denoted by $\hat{\mathcal{G}}_1$. Note that a nuclear Newton graph fulfils the *A-property* (but certainly not the *E-property*). Consequently, a graph of the type $\hat{\mathcal{G}}_1$ is neither a Newton graph, nor equivalent with a graph $\mathcal{G}(f), f \in \check{E}_r$. Nevertheless, nuclear Newton graphs will play an important role because, in a certain sense, they "generate" certain structurally stable Newton flows. This will be explained in the sequel.

3 Nuclear elliptic Newton flow

Throughout this section, let f be an elliptic function with -viewed to as to a function on $T = T(\Lambda(\omega_1, \omega_2))$ - only one zero and one pole, both of order $r, r \geqslant 2$. Our aim is to derive the result on the corresponding (so-called nuclear) Newton flow $\overline{\overline{\mathcal{N}}}(f)$ that was already announced in [2], Remark 5.8. To be more precise:

> " All nuclear Newton flows -of any order r- are conjugate , in particular each of them has precisely two saddles (simple) and there are no saddle connections".

When studying -up to conjugacy- the flow $\overline{\overline{\mathcal{N}}}(f)$, we may assume (cf. Subsubsection 1.1.3) that $\omega_1 = 1, \omega_2 = i$, thus $\Lambda = \Lambda_{1,i}$. In particular, the period pair $(1, i)$ is reduced. We represent f (and thus $\overline{\overline{\mathcal{N}}}(f)$), by the Λ-classes $[a], [b]$, where a resp. b stands for the zero,

resp. pole, for f, situated in the period parallelogram $P(= P_{1,i})$. Due to (2), (3) we have:

$$b = a + \frac{\lambda_0}{r}.$$

We may assume that a, b are not on the boundary ∂P of P. Since the period pair $(1, i)$ is reduced, the images under f of the P-sides γ_1 and γ_2 are closed Jordan curves (use the explicit formula for λ^0 as presented in Footnote 3). From this, we find that the winding numbers $\eta(f(\gamma_1))$ and $\eta(f(\gamma_2))$ can -a priori- only take the values -1, 0 or +1. The combination $(\eta(f(\gamma_1)), \eta(f(\gamma_2))) = (0, 0)$ is impossible (because $a \neq b$). The remaining combinations lead, for each value of $r = 2, 3, \cdots$, to eight different values for b each of which giving rise, together with a, to eight pairs of classes $\bmod \Lambda$ that fulfil (2), determining flows in $N_r(\Lambda)$, compare Fig. 8, where we assumed -under a suitable translation of P-that $a = 0$.

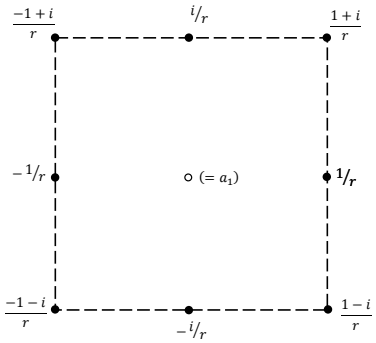

Figure 8: Eight pairs (a, b) determining a priori possible nuclear flows in $N_r(\Lambda_{1,i})$.

Note that the derivative f' is elliptic of order $r + 1$. Since there is on P only one zero for f (of order r), the function f has two critical points, i.e., saddles for $\overline{\overline{\mathcal{N}}}(f)$, counted by multiplicity.

The eight pairs (a, b) that possibly determine a nuclear Newton flow are subdivided into two classes, each containing four configurations (a, b): (see Fig.9)

Class 1: $a = 0$, b on a side of the period square P.
Class 2: $a = 0$, b on a diagonal of the period square P, but not on ∂P.

Apparently, two nuclear Newton flows represented by configurations in the same class are related by a *unimodular* transformation on the period pair $(1, i)$, and are thus conjugate, see Subsubsection 1.1.3. So, it is enough to study nuclear Newton flows, possibly represented by $(0, \frac{1}{r})$ or $(0, \frac{1+i}{r})$.

The configuration $(a, b), a = 0, b = \frac{1}{r}$:
The line ℓ_1 between 0 and 1, and the line ℓ_2 between $\frac{1}{i}$ and $1 + \frac{1}{i}$, are axes of mirror symmetry with respect to this configuration (cf. Fig.10-(i)). By the aid of this symmetry and using the double periodicity of the supposed flow , it is easily proved that this configuration can not give rise to a desired nuclear Newton flow.

The configuration $(a, b), a = 0, b = \frac{1+i}{r}$:
The line ℓ between 0 and $\frac{1+i}{2}$ is an axis of mirror symmetry with respect to this configuration

(cf. Fig.10-(ii)). So the two saddles of the possible nuclear Newton flow are situated either on the diagonal of P through $\frac{1+i}{r}$, or not on this diagonal but symmetric with respect to ℓ_1. The first possibility can be ruled out (by the aid of the symmetry w.r.t. ℓ and using he double periodicity of the supposed flow). So it remains to analyze the second possibility. (Note that only in the case where $r = 2$, also the second diagonal of P yields an axis of mirror symmetry).

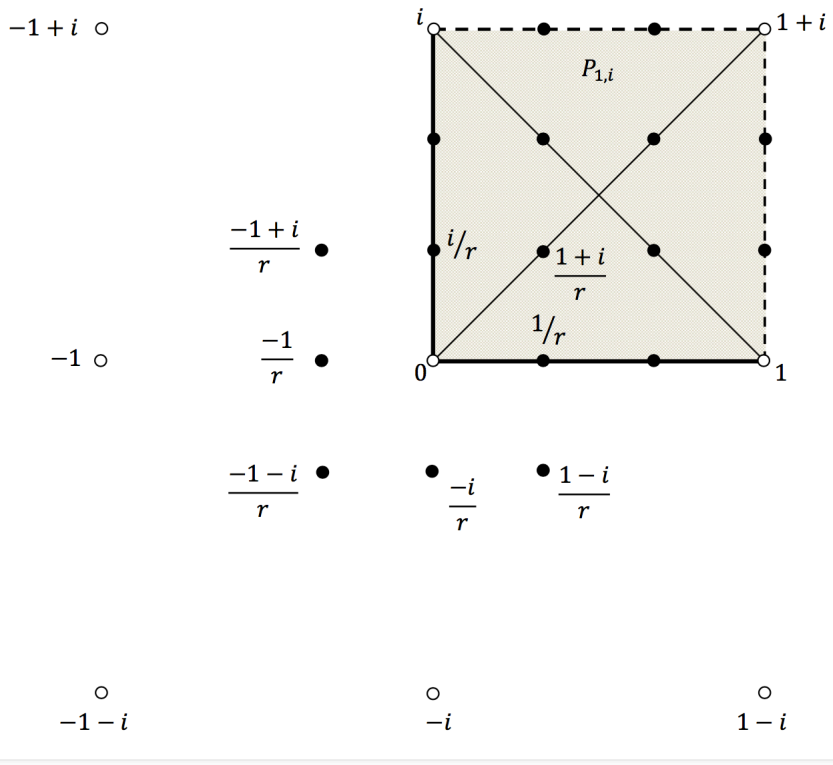

Figure 9: The two classes of pairs $(a, b) = (0, \bullet)$ on $P_{1,i}$.

We focus on Fig.11, where the only relevant configuration determining a (planar) flow $\overline{\overline{\mathcal{N}}}(f)$, is depicted. By symmetry, the ℓ-segments between 0 and $\frac{1+i}{r}$, and between $\frac{1+i}{r}$ and $(1+i)$ are $\overline{\overline{\mathcal{N}}}(f)$-trajectories connecting the pole $\frac{1+i}{r}$, with the zeros 0 and $(1+i)$. Since on the $\overline{\overline{\mathcal{N}}}(f)$-trajectories the $\arg(f)$ values are constant, we may arrange the argument function on $\mathbb{C}$ such that on the segment between $\frac{1+i}{r}$ and $1+i$ we have $\arg(f)= 0$. We put $\arg f(\sigma_1)= \alpha$, thus $0 < \alpha < 1$ and $\arg f(\sigma_2)= -\alpha$. Note that at the zero / pole for f, each value of $\arg(f)$ appears r times on equally distributed incoming (outgoing) $\overline{\overline{\mathcal{N}}}(f)$-trajectories. By the aid of this observation, together with the symmetry and periodicity of f, we find out that the phase portrait of $\overline{\overline{\mathcal{N}}}(f)$ is as depicted in Fig.11, where box stands for the (constant values of $\arg(f)$ on the unstable manifolds of $\overline{\overline{\mathcal{N}}}(f)$. In particular, there are no saddle connections.

Remark 3.1. *Canonical form of the phase portrait of a nuclear Newton flow*
The qualitative features of the phase portrait of $\overline{\overline{\mathcal{N}}}(f)$ in Fig.11 rely on the values of r and

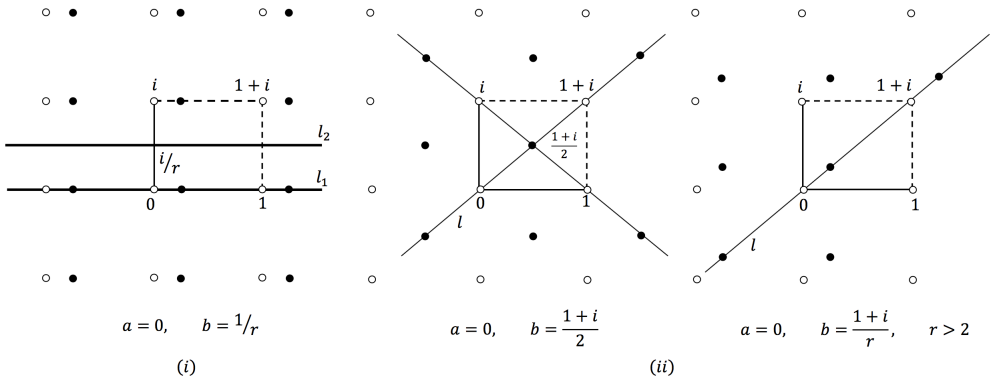

Figure 10: Axes of window symmetry for the configuration $(a, b)(= (0, \bullet))$.

α. Put $\beta = \frac{1}{2} + \alpha - \frac{1}{r}$ and $\gamma = \frac{1}{r} - 2\alpha$. Since all angles α, β and γ are strictly positive, we have $0 < \alpha < \frac{1}{2r}$. Note that if $r = 2$, by symmetry w.r.t. both the diagonals of P, we have $\alpha = \beta = \frac{1}{8}; \gamma = \frac{1}{4}$, see Fig.12; in this case $\overline{\overline{\mathcal{N}}}(f)$ is just $\overline{\overline{\mathcal{N}}}(\wp)$, with $\wp$ the Weierstrass' $\wp$-function (lemniscate case, cf. [1]).

Altogether we conclude:

Lemma 3.2. *All nuclear elliptic Newton flows of the same order r are mutually conjugate.*

For f an elliptic function of order r with - on T - only one zero and pole we now define:

Definition 3.3. $\mathcal{H}_r(f)$ is the graph on T with as vertex, edges and face respectively:
- the zero for f on T (as atractor for $\overline{\overline{\mathcal{N}}}(f)$);
- the unstable manifolds for $\overline{\overline{\mathcal{N}}}(f)$ at the two critical points for f;
- the basin of repulsion for $\overline{\overline{\mathcal{N}}}(f)$ of a pole for f on T (as a repellor for $\overline{\overline{\mathcal{N}}}(f)$).

From Fig.11 it is evident that $\mathcal{H}_r(f)$ is a cellularly embedded pseudo graph (loops and multiple edges permitted). This graph is referred to as to the *nuclear Newton graph* for $\overline{\overline{\mathcal{N}}}(f)$. By Lemma 3.2, the graphs $\mathcal{H}_r(f)$, are - up to equivalency - unique, and will be denoted by $\mathcal{H}_r$ (compare the comment on Definition 2.5).

If a, b (both in $P(= P_{1,i})$) are of Class 2 (i.e., the configuration (a, b) determines a nuclear flow with a and b as zero resp. pole of order r), we introduce the doubly periodic functions:

$$\Psi_a(z) = \sqrt{\sum_{\omega \in \Lambda} |z - a - \omega|^{-(4r-4)}}; \quad \Psi_b(z) = \sqrt{\sum_{\omega \in \Lambda} |z - b - \omega|^{-(4r-4)}}, \tag{6}$$

where the summation takes place over all points in lattice $\Lambda(= \Lambda_{1,i})$.

We define the planar flow $\underline{\mathcal{N}}(f)$ by:

$$\frac{dz}{dt} = -\Psi_a(z)\Psi_b(z)(1 + |f(z)|^4)^{-1}\overline{f'(z)}f(z) \tag{7}$$

Lemma 3.4. *The flow $\underline{\mathcal{N}}(f)$ is smooth on $\mathbb{C}$ and exhibits the same phase portrait as $\overline{\mathcal{N}}(f)$, but, its attractors (at zeros for f) and its repellors (at the poles for f) are all generic, i.e. of the hyperbolic type.*

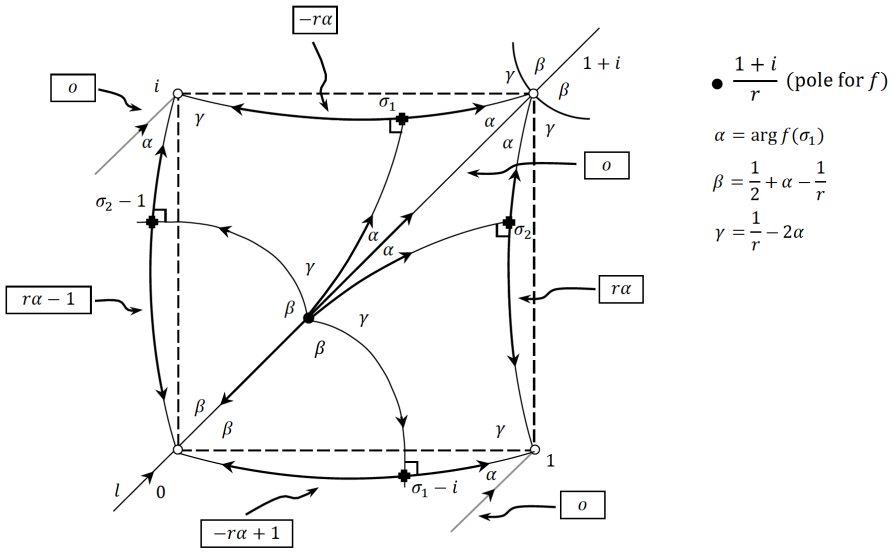

Figure 11: The phase portrait of a nuclear Newton flow of order $r > 2$.

Proof. Since $r \geqslant 2$ (thus $4r - 4 \geqslant 4$), series of the type as under the square root in (6) are uniform convergent in each compact subset of $\mathbb{C}\backslash(a + \Lambda \cup b + \Lambda)$. From this, together with the smoothness of $\overline{\mathcal{N}}(f)$ on $\mathbb{C}$, it follows that $\underline{\mathcal{N}}(f)$ is smooth outside the union of $a + \Lambda$ and $b + \Lambda$. Special attention should be paid to the lattice points. Here the smoothness of $\underline{\mathcal{N}}(f)$ as well as the genericity of its attractors and repellors follows by a careful (but straightforward) analysis of the local behaviour of $\underline{\mathcal{N}}(f)$ around these points; compare the explicit expression for $\overline{\mathcal{N}}(f)$ in Footnote 1 and note that zeros and poles are of order r. Since outside their equilibria $\underline{\mathcal{N}}(f)$ and $\overline{\mathcal{N}}(f)$ are equal -up to a strictly positive factor- their portraits coincide. □

Corollary 3.5. *All nuclear Newton flows of arbitrary order are mutually conjugate.*

Proof. Let $\underline{N}(f)$ be arbitrary. Because all its equilibria are generic and there are no saddle connections, this flow is C^1-structurally stable. The embedded graph $\mathcal{H}_r(= \mathcal{H}_r(f))$, together with its geometrical dual $\mathcal{H}_r(f)^*$, forms the so-called distinguished graph that determines - up to an orientation preserving homeomorphism - the phase portrait of $\underline{N}(f)$ (cf. [10], [11] and Subsubsection 1.2.3). This distinghuished graph is extremely simple, giving rise to only four distinghuished sets (see Fig.11). This holds for any flow of the type $\underline{N}(f)$. Now, application of Peixoto's classification theorem for C^1-structurally stable flows on T yields the assertion. □

We end up with a comment on the nuclear Newton graph $\mathcal{H}(f_{\omega_1,\omega_2})$, $\mathrm{Im}\frac{\omega_2}{\omega_1} > 0$, where (ω_1, ω_2), is related to the period pair $(1, i)$ by the unimodular transformation

$$M = \begin{pmatrix} p_1 & q_1 \\ p_2 & q_2 \end{pmatrix}, \quad p_1 q_2 - p_2 q_1 = +1.$$

Thus (p_1, p_2) and (q_1, q_2) are co-prime, and

$$\omega_1 = p_1 + p_2 i, \quad \omega_2 = q_1 + q_2 i.$$

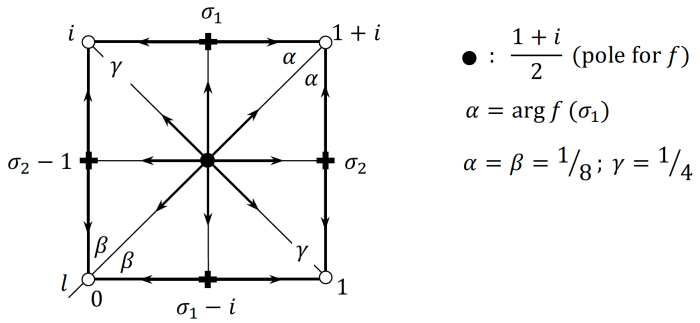

Figure 12: The canonical nuclear Newton flow of order $r = 2$.

Our aim is to describe $\mathcal{H}(f_{\omega_1,\omega_2})$ as a graph on the canonical torus $T(= T_{1,i})$. In view of Lemma 3.2, the two edges of $\mathcal{H}(f_{\omega_1,\omega_2})$ are closed Jordan curves on T , corresponding to the unstable manifolds of $\overline{\mathcal{N}}(f_{\omega_1,\omega_2}))$ at the two critical points for f that are situated in the period parallelogram P_{ω_1,ω_2}. These unstable manifolds connect $a(= 0)$ with $p_1 + p_2 i$, and $q_1 + q_2 i$ respectively. Hence, one of the $\mathcal{H}(f_{\omega_1,\omega_2})$-edges wraps p_1-times around T in the direction of the period 1 and p_2-times around T in the direction of the period i, whereas the other edge wraps q_1-times around this torus in the 1-direction respectively q_2-times in the i-direction. See also Fig.13, where we have chosen for f the Weierstrass $\wp$-function (lemniscate case), i.e. $r = 2$, $a = 0$ and $\omega_1 = 3 + i, \omega_2 = 2 + i$. Compare also Fig.12, case $r = 2$.

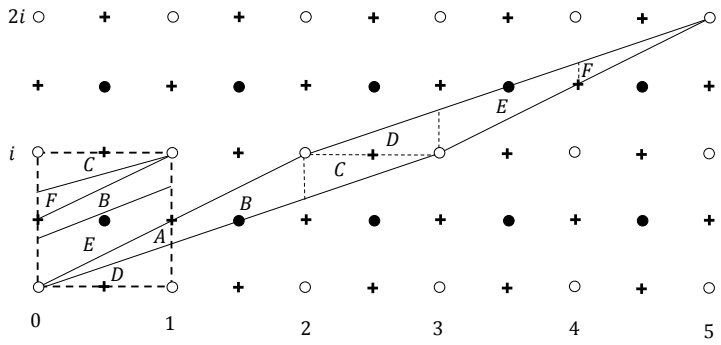

Figure 13: The nuclear Newton graph $\mathcal{H}(\wp_{3+i,2+i})$ on the torus $T(= T_{1,i})$.

4 The bifurcation & creation of elliptic Newton flows

In this section we discuss the connection between pseudo Newton graphs and Newton flows. In order not to blow up the size of our study, we focus - after a brief introduction - on the cases $r = 2, 3$. However, even from these simplest cases we get some flavor of what we may expect when dealing with a more general approach.

We consider functions $g \in E_r$ with r simple zeros and only one pole (of order r); such functions exist, compare Subsubsection 1.1.1. The set of all these functions is denoted by

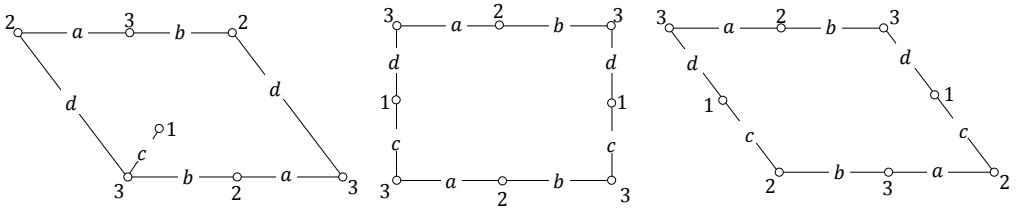

Figure 14: The three different pseudo Newton graphs $\check{\mathcal{G}}_3$, $\hat{\mathcal{G}}_3$.

E_r^1 and will be endowed with the relative topology induced by the topology τ_0 on E_r. Since the derivative g' of g is elliptic of order $r+1$, the zeros for g being simple, there are $r+1$ critical points for g (counted by multiplicity).

We consider the set N_r^1 of all toroidal Newton flows $\overline{\overline{\mathcal{N}}}(g)$. Such a flow is C^1-structurally stable (thus also τ_0-structurally stable) if and only if: (cf. subsection 1.1.4 and [10], [11])

1. All saddles are simple (thus generic).
2. There are no "saddle connections".
3. The repellor at the pole for g is generic.

In general none of these conditions is fulfilled. We overcome this complication as follows:
ad 1. Under suitably chosen - but arbitrarily small - perturbations of the zeros and poles of g, thereby preserving their multiplicities, $\overline{\overline{\mathcal{N}}}(g)$ turns into a Newton flow with only simple (thus $r+1$) saddles (cf. [2], Lemma 5.7, case $A = r, B = 1$).
ad 2. Possible saddle connections can be broken by adding to g a suitably chosen, but arbitrarily small constant (cf.[2], proof of Theorem 5.6 (2)).
ad 3. With the aid of a suitably chosen additional damping factor to $\overline{\overline{\mathcal{N}}}(g)$, the pole of g may be viewed to as generic for the resulting flow; compare the proof of Lemma 3.4. (Note that the simple zeros for g yield already generic equilibriae).

This opens the possibility to adapt g and $\overline{\overline{\mathcal{N}}}(g)$ in such a way that for almost all functions g the flow $\overline{\overline{\mathcal{N}}}(g)$ is structurally stable (see Subsubsection 1.1.4, and Theorem 5.6 in [2]). More formally:

The set $\underline{\underline{E}}_r^1$ of functions g in E_r^1, with $\overline{\overline{\mathcal{N}}}(g)$ structurally stable, is τ_0-open and -dense in E_r^1.

From now on, we assume that $\overline{\overline{\mathcal{N}}}(g)$ is structurally stable and define the multi graph $\mathcal{G}_r(g)$ on T as follows:
- Vertices: r zeros for g (i.e., stable star nodes for $\overline{\overline{\mathcal{N}}}(g)$).
- Edges: $r+1$ unstable manifolds at the critical points for g (orthogonal saddles for $\overline{\overline{\mathcal{N}}}(g)$).
- Face: the basin of repulsion of the unstable star node at the pole for g.
Note that $\mathcal{G}_r(g)$ has no loops (since the zeros for g are simple).

It is easily seen that $\mathcal{G}_r(g)$ is cellularly embedded (cf. [3], proof of Lemma 2.9).

Because $\mathcal{G}_r(g)$ has only one face, the geometrical dual $\mathcal{G}_r(g)^*$ admits merely loops and the Π-walk for the $\mathcal{G}_r(g)$-face consists of $2(r+1)$ edges, each occurring twice, be it with opposite orientation; here the orientation on the Π-walk is induced by the anti-clockwise orientation on the embedded $\mathcal{G}_r(g)^*$-edges at the pole for g. In the case where $\mathcal{G}_r(g)$ admits a vertex of degree 1, we delete this vertex together with the adjacent edge, resulting into a cellularly embedded graph on $r-1$ vertices, r edges and only one face. If this graph has a vertex of degree 1, we repeat the procedure, and so on. The process stops after $L\,(< r-1)$ steps, resulting into a connected, cellularly embedded muligraph of the type $\hat{\mathcal{G}}_\rho, \rho = r-L, 2 \leqslant \rho \leqslant r$.

Now, we raise the question whether the graphs obtained in this way are indeed pseudo Newtonian, i.e., do they originate from a Newton graph? And even so, can all pseudo Newton graphs be represented by elliptic Newton flows?

In the sequel we give an (affirmative) answer to these questions only in the cases $r = 2$ and $r = 3$.

Lemma 4.1. *If $r = 2$ or 3, then the graph $\mathcal{G}_r(g)$, $g \in \underline{E}^1_r$, is a pseudo Newton graph $\check{\mathcal{G}}_r$.*

Proof. Firstly, note that the proof of Lemma 2.1 does not rely on the fact that $\hat{\mathcal{G}}_\rho$ originates from Newton graphs, but merely on the cellularity of $\hat{\mathcal{G}}_\rho$ in combination with the property that $\#\{\text{edges}\} = 1 + \#\{\text{vertices}\}$.
Case $r = 2$: By Corollary 2.2 of Lemma 2.1 we know: $\hat{\mathcal{G}}_2$ $(= \check{\mathcal{G}}_2)$ is unique (up to equivalency). So, $\mathcal{G}_2(g)$ has the same topological type as $\hat{\mathcal{G}}_2$ and originates from a Newton graph (compare Fig.3 and Fig.6a_1, where all subwalks W_i admit only one edge).
Case $r = 3$: If $\mathcal{G}_3(g)$ has a vertex v_1 of degree 1, the graph obtained by deleting v_1 together with the adjacent edge c is a cellularly embedded graph in T with two vertices and three edges and must $\hat{\mathcal{G}}_2$. So $\mathcal{G}_3(g)$ is of the form Fig.14(a).

If $\mathcal{G}_3(g)$ has no vertex of degree 1, this graph is of type $\check{\mathcal{G}}_3$, and thus - by Corollary 2.2 - either of the form as depicted in Fig.14 (b), or Fig.14 (c).

So, we find that $\mathcal{G}_3(g)$ takes, a priori, the three possible forms in Fig.14, where the values of degree v_i discriminate between these possibilities. Recall that these three graphs originate from Newton graphs. □

The reasoning in the above Case $r = 3$ does *not* imply that each of the graphs in Fig.14 can be realized by a Newton flow. So we need:

Lemma 4.2. *If $r = 2$ or 3, then each pseudo Newton graph of the type $\check{\mathcal{G}}_r$ or $\hat{\mathcal{G}}_r$ can be represented as $\mathcal{G}_r(g)$, $g \in \underline{E}^1_r$.*

Proof. $\underline{r = 2}$: Follows from Lemma 4.1.
$\underline{r = 3}$: In Fig.16 we consider the local phase portrait of $\overline{\mathcal{N}}(f)$ around the zero $v(= 1+i)$ for f. Compare Fig.11 and note that the zeros for f are star nodes for $\overline{\mathcal{N}}(f)$. Since $\alpha+\gamma = \frac{1}{r}-\alpha$ and $\alpha+\beta+\gamma = \frac{1}{2}$ we have $\beta > \frac{1}{2r}$ so that the angle $\beta+\beta$ spans an arc greater than $\frac{1}{r}(= \frac{1}{3})$. Now the idea is:

To split off from the 3^{rd} order zero v for f a simple zero (v_1) "Step 1", and thereupon, to split up the remaining double zero $(v_1^{'})$ into two simple ones (v_2, v_3) "Step 2", in such a way that by an appropriate strategy, the resulting functions give rise to Newton flows with associated graphs, determining each of the three possible types in Fig.14.
Ad Step 1 : We perturb the original function f into an elliptic function g with one simple (v_1) and one double $(v_1^{'})$ zero (close to each other), and one third order pole w_1 (thus close[11]

[11] Use property (2).

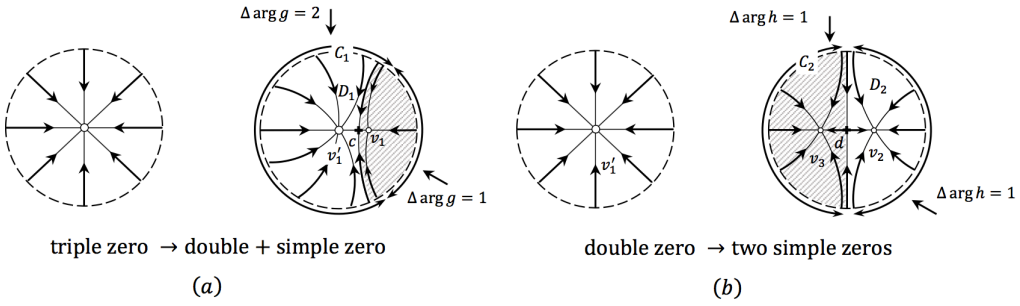

Figure 15: Splitting zeros

to the third order pole w of f). The original flow $\overline{\overline{\mathcal{N}}}(f)$ perturbs into a flow $\overline{\overline{\mathcal{N}}}(g)$ with v_1 and $v_1^{'}$ as attractors and w_1 as repellor. When v_1 tends to $v_1^{'}$, the perturbed function g will tend to f, and thus the perturbed flow $\overline{\overline{\mathcal{N}}}(g)$ to $\overline{\overline{\mathcal{N}}}(f)$, cf. Subsubsection 1.1.2. In particular, when the splitted zeros are sufficiently close to each other and the circle C_1 that encloses an open disk D_1 with center $v_1^{'}$, is chosen sufficiently small, C_1 is a global boundary (cf.[7]) for the perturbed flow $\overline{\overline{\mathcal{N}}}(g)$. It follows that, apart from the equilibria v_1 and $v_1^{'}$ (both of Poincaré index 1) the flow $\overline{\overline{\mathcal{N}}}(g)$ exhibits on D_1 one other equilibrium (with index -1): a simple saddle, say c (cf. [5]). From this, it follows (cf. Subsubsection 1.1.1) that the phase portrait of $\overline{\overline{\mathcal{N}}}(g)$ around v_1 and $v_1^{'}$ is as sketched in Fig.15-(a), where the local basin of attraction for v_1 is shaded and intersects C_1 under an arc with length approximately $\frac{1}{3}$.

On the (compact!) complement $T\backslash D_1$ this flow has one repellor (w_1) and two saddles. The repellor may be considered as hyperbolic (by the suitably chosen damping factor, compare the proof of Lemma 3.4), whereas the saddles are distinct and thus simple (because $\overline{\overline{\mathcal{N}}}(f)$ has two simple saddles, say σ_1, σ_2, depending continuously on v_1 and $v_1^{'}$). Hence, the restriction of $\overline{\overline{\mathcal{N}}}(g)$ to $T\backslash D_1$ is ε-structurally stable (cf. [10]). So, we may conclude that, if v_1 (chosen sufficiently close to $v_1^{'}$) turns around $v_1^{'}$, the phase portraits outside D_1 of the perturbed flows undergo a change that is negligible in the sense of the C^1-topology. Therefore, we denote the equilibria of $\overline{\overline{\mathcal{N}}}(g)$ on $T\backslash D_1$ by w_1, σ_1, σ_2 (i.e., without reference to v_1). We move v_1 around a small circle, centered at $v_1^{'}$ and focus on two positions (I, II) of v_1, specified by the position of v_1 w.r.t. the symmetry axis ℓ. See Fig.16 in comparison with Fig.17, where we sketched some trajectories of the phase portraits of $\overline{\mathcal{N}}(g)$ on D_1.

Ad Step 2 : We proceed as in Step 1. Splitting $v_1^{'}$ into v_2 and v_3 (sufficiently close to each other) yields a perturbed elliptic function h, and thus a perturbed flow $\overline{\overline{\mathcal{N}}}(h)$. Consider a circle C_2, centered at the mid-point of v_2 and v_3, that encloses an open disk D_2 containing these points. If we choose C_2 sufficiently small, it is a global boundary of $\overline{\overline{\mathcal{N}}}(h)$. Reasoning as in Step 1, we find out that $\overline{\overline{\mathcal{N}}}(h)$ has on D_2 two simple attractors (v_2 , v_3) and one simple saddle: d (close to the mid point of v_2 and v_3; compare Fig.15-(b)), where the local basin of attraction for v_3 is shaded and intersects C_2 under an arc with length approximately $\frac{1}{2}$. Moreover, as for $\overline{\overline{\mathcal{N}}}(g)$ in Step 1, the flow $\overline{\overline{\mathcal{N}}}(h)$ is ε-structurally stable outside D_2. So, we may conclude that, if v_2 and v_3 turn (in diametrical position) around their mid-point, the phase portraits outside D_2 of the perturbed flows undergo a change that is negligible in the sense of C^1-topology. Therefore, we denote the equilibria of $\overline{\overline{\mathcal{N}}}(h)$ on $T\backslash D_2$ by v_1, w_1, c, σ_1,

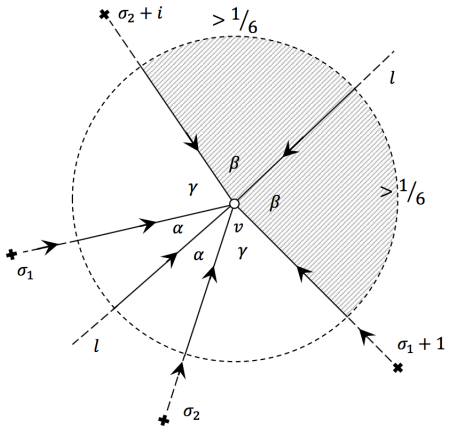

Figure 16: Local phase portrait of $\overline{\overline{\mathcal{N}}}(f)$ around the zero $v(= 1 + i)$ for f; $r = 2$.

and σ_2 (i.e., without reference to v_2 and v_3).

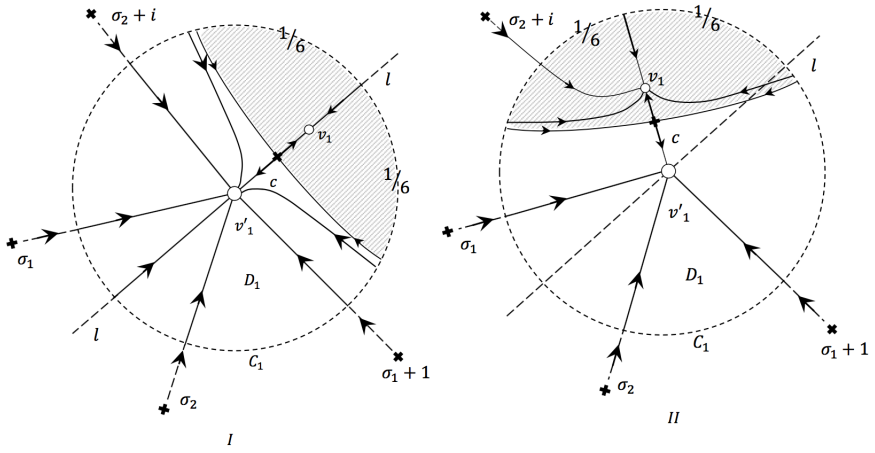

Figure 17: Phase portraits for $\overline{\overline{\mathcal{N}}}(g))$ on D_1.

Finally, for v_1 in the position of Fig.17-(I) we choose the pair (v_2,v_3) as in Fig.18-I; and for v_1 in the position of Fig.17-(II), we distinguish between two possibilities: Fig.18-IIa or Fig.18-IIb. Note that, with these choices of v_1, v_2, v_3 each of the obtained functions has three simple zeros and one triple pole. Moreover, the four saddles are simple and not connected, whereas the three zeros are simple as well. So the graph of the associated Newton flow is well defined and has only one face, four edges and three vertices. Recall that the various values of degree v_i discriminate between the three possibilities for the graphs of type $\check{\mathcal{G}}_3$). Now inspection of Fig.18 yields the assertion. □

Up till now, we paid attention to pseudo Newton graphs with only one face (i.e., of type $\check{\mathcal{G}}$ or $\hat{\mathcal{G}}$.). If $r = 2$, these are the only possibilities.

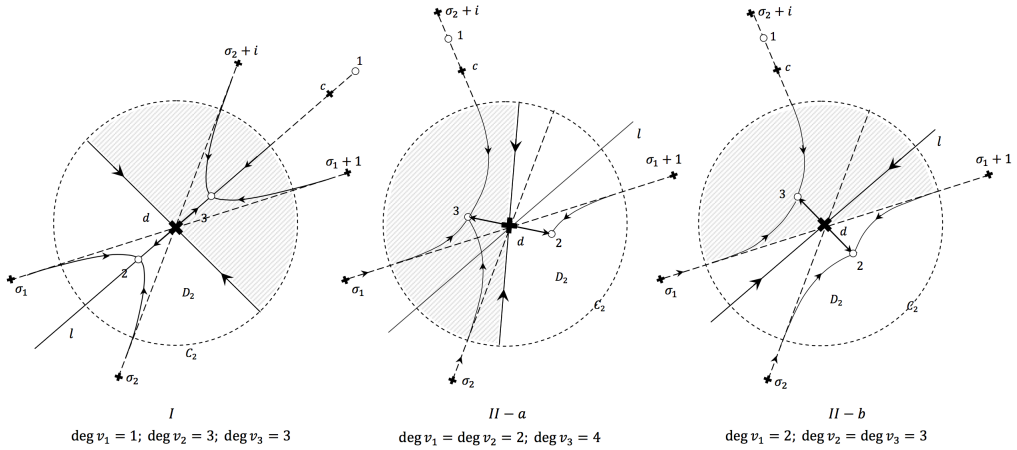

Figure 18: The three phase portraits for $\overline{\overline{\mathcal{N}}}(h))$ on D_2.

If $r = 3$, there are also pseudo Newton graphs (denoted by $\underline{\mathcal{G}}$) with two faces and angles summing up to 1 or 2. When the boundaries of any pair of the original $\mathcal{G}_3$-faces have a subwalk in common, these walks have length 1 or 2. (Use the A-property and compare Fig.4). So, when two $\mathcal{G}_3$-faces are merged, the resulting $\underline{\mathcal{G}}$-face admits *either* only vertices of degree $\geqslant 2$ *or* one vertex of degree 1[12]. From now on, we focus on the Newton graphs as exposured in Fig.4 (i),(iv) [since all other Newton graphs (in this figure) can be dealt with in the same way, there is no loss of generality]. Then the two $\underline{\mathcal{G}}$-faces under consideration are $\underline{F}_7$ (:= $F_{4,6}$) and $\underline{F}_8 := F_5$; see Fig.19 (in comparison with Fig.4 (i),(iv)).

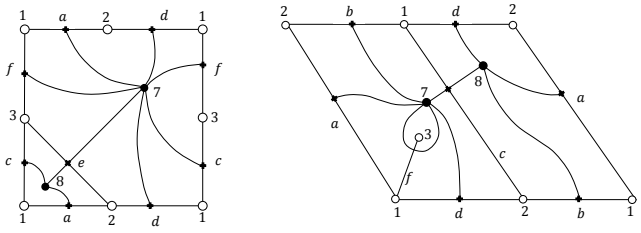

Figure 19: The graph $\underline{\mathcal{G}} \wedge \underline{\mathcal{G}}^*$.

We consider the common refinement $\underline{\mathcal{G}} \wedge \underline{\mathcal{G}}^*$ of $\underline{\mathcal{G}}$ and its dual $\underline{\mathcal{G}}^*$. Following Peixoto [10], [11] we claim that $\underline{\mathcal{G}} \wedge \underline{\mathcal{G}}^*$ determines a C^1-structurally stable toroidal flow $X(\underline{\mathcal{G}})$ with canonical regions as depicted[13] in Fig.20. As equilibria for $X(\underline{\mathcal{G}})$ we have: three stable and two unstable proper nodes (corresponding to the $\underline{\mathcal{G}}$-resp. $\underline{\mathcal{G}}^*$-vertices) and five orthogonal saddles (corresponding to the pairs (e, e^*) of $\underline{\mathcal{G}}$- and $\underline{\mathcal{G}}^*$-edges).

Argueing basically as in the proof of Theorem 4.1 from our paper [3] , it can be shown that $X(\underline{\mathcal{G}}))$ is equivalent with an elliptic Newton flow generated by a function on three

[12]The E-property holds not always for $\underline{\mathcal{G}}$: Only if there is a $\underline{\mathcal{G}}$-vertex of degree 1, the dual $\underline{\mathcal{G}}^*$ admits a *contractible* loop (corresponding with the edge adjacent to this vertex); all other $\underline{\mathcal{G}}^*$-loops- if there are any- are *non-contractible*.

[13]In the terminology used in [10], the canonical region in the r.h.s. of Fig.20 is of Type 3, whereas the other two regions are of Type 1.

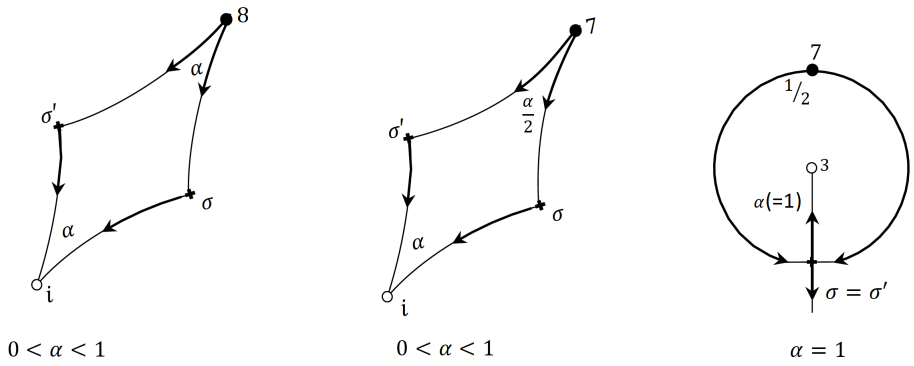

Figure 20: The various appearances of the canonical regions of $\mathcal{X}(\underline{\mathcal{G}})$.

simple zeros, one double and one simple pole and five simple critical points; compare[14] Fig.10. As an elliptc Newton flow, $X(\underline{\mathcal{G}})$ is not (τ_0-)structurally stable, since $\underline{\mathcal{G}}$ is not Newtonian, compare Subsubsection 1.2.2. However, by the aid of a suitably chosen damping factor, compare Lemma 3.4 (preambule), and within the class of all elliptic Newton flows generated by functions on three simple zeros, on one double and one simple pole and on five simple critical points, the flow $X(\underline{\mathcal{G}})$ is structurally stable w.r.t. the relative topology τ_0.

Altogether, we find:

Theorem 4.3. *Any pseudo Newton graph of order $r, r = 2, 3$ represents an elliptic Newton flow. In particular, the 3^{rd} order nuclear Newton flow "creates" - by splitting up zeros/ poles ("bifurcation")- all, up to duality and topological equivalency, structurally stable elliptic Newton flows of order 3.*

References

[1] Abramowitz, A., Stegun, I.A. (eds): *Handbook of Mathematical Functions. Dover Publ. Inc. (1965).*

[2] Helminck, G.F., Twilt, F.: *Newton flows for elliptic functions I, Structural stability: characterization & genericity*, arXiv: 1609.01267v1 [math.DS].

[3] Helminck, G.F., Twilt, F.: *Newton flows for elliptic functions II, Structural stability: classification & representation*, arXiv: 1609.01323v1 [math.DS].

[4] Helminck, G.F., Twilt, F.: *Newton flows for elliptic functions III, Classification of 3^{rd} order Newton graphs*, arXiv: 1609.01335v1 [math.DS].

[5] Guillemin, V., Pollack, A. :*Differential Topology*, Prentice Hall Inc. (1974).

[6] Hirsch, M.W.: *Differential Topology. Springer Verlag (1976).*

[7] Jongen, H.Th., Jonker, P., Twilt, F.: *Nonlinear Optimization in $\mathbb{R}^n$: Morse Theory, Chebyshev Approximation, Transversality, Flows, Parametric Aspects. Kluwer Ac. Publ., Dordrecht, Boston (2000).*

[14] The picture in the r.h.s. of Fig.20 corresponds to a canonical region in the $\underline{\mathcal{G}}$-face with angles summing up to 1, determining the simple pole for $X(\underline{\mathcal{G}})$, compare also Fig.1. The other two pictures correspond to the $\underline{\mathcal{G}}$-face with angles summing up to 2, determining the double pole for $X(\underline{\mathcal{G}})$.

[8] Markushevich, A.I.: *Theory of Functions of a Complex Variable, Vol. III, Prentice Hall (1967).*

[9] Mohar, B.;Thomassen, C. : *Graphs on surfaces.* John Hopkins Studies in the Mathematical Sciences. John Hopkins University Press, Baltimore, MD, 2001.

[10] Peixoto, M.M.: *Structural stability on two-dimensional manifolds. Topology* 1, pp. 101-120 (1962).

[11] Peixoto, M.M.: *On the classification of flows on 2-manifolds. In:Dynamical Systems, M.M. Peixoto, ed., pp. 389-419, Acad. Press, NewYork (1973)* .